Protist, Vol. 157, 401—419, August 2006
http://www.elsevier.de/protis
Published online date 7 August 2006

Protist

ORIGINAL PAPER

Hatena arenicola gen. et sp. nov., a Katablepharid Undergoing Probable Plastid Acquisition

Noriko Okamoto[2], and Isao Inouye[1]

Graduate School of Life and Environmental Sciences, University of Tsukuba, 1-1-1, Tennodai, Tsukuba, Ibaraki 305-8572, Japan

Submitted February 27, 2006; Accepted May 27, 2006
Monitoring Editor: Robert A. Andersen

***Hatena arenicola* gen. et sp. nov., an enigmatic flagellate of the katablepharids, is described. It shows ultrastructural affinities to the katablepharids, including large and small ejectisomes, cell covering, and a feeding apparatus. Although molecular phylogenies of the 18S ribosomal DNA support its classification into the katablepharids, the cell is characterized by a dorsiventrally compressed cell shape and a crawling motion, both of which are unusual within this group. The most distinctive feature of *Hatena arenicola* is that it harbors a *Nephroselmis* symbiont. This symbiosis is distinct from previously reported cases of ongoing symbiosis in that the symbiont plastid is selectively enlarged, while other structures such as the mitochondria, Golgi body, cytoskeleton, and endomembrane system are degraded; the host and symbiont have developed a morphological association, i.e., the eyespot of the symbiont is always at the cell apex of *Hatena arenicola*; and only one daughter cell inherits the symbiont during cell division, resulting in a symbiont-bearing green cell and a symbiont-lacking colorless cell. Interestingly, the colorless cells have a feeding apparatus that corresponds to the location of the eyespot in symbiont-bearing cells, and they are able to feed on prey cells. This indicates that the morphology of the host depends on the presence or absence of the symbiont. These observations suggest that *Hatena arenicola* has a unique "half-plant, half-predator" life cycle; one cell divides into an autotrophic cell possessing a symbiotic *Nephroselmis* species, and a symbiont-lacking colorless cell, which later develops a feeding apparatus de novo. The evolutionary implications of *Hatena arenicola* as an intermediate step in plastid acquisition are discussed in the context of other examples of ongoing endosymbioses in dinoflagellates.**

Key words: *Hatena arenicola*; Katablepharidophyta/Kathablepharida; *Nephroselmis* symbiont; plant evolution; plastid acquisition via secondary endosymbiosis; ultrastructure.

Abbreviations: EM = electron microscopy; ER = endoplasmic reticulum; ICBN = International Code of Botanical Nomenclature; ICZN = International Code of Zoological Nomenclature; LM = light microscopy; SEM = scanning electron microscopy; SSU rDNA = small subunit ribosomal DNA; TEM = transmission electron microscopy.

[1]Corresponding author;
fax +81 29 853 4533
e-mail iinouye@sakura.cc.tsukuba.ac.jp (I. Inouye).
[2]Current address: School of Botany, University of Melbourne, Parkville, Victoria, Australia.

doi:10.1016/j.protis.2006.05.011

Introduction

Eukaryotes are currently classified into five or six supergroups (Baldauf et al. 2000; Baldauf 2003; Bapteste et al. 2002; Nozaki et al. 2003; Simpson and Roger 2002), and eukaryotic autotrophs (e.g., plants and algae) randomly scatter across those supergroups. Eukaryotic autotrophs comprise nine distinct divisions in cell architecture, and this enormous diversity is explained by several endosymbiotic events (Bhattacharya et al. 2004; Falkowski et al. 2004; McFadden 2001). It is widely accepted that a primary endosymbiosis between a eukaryote and a cyanobacterial symbiont gave rise to the three extant primary eukaryotic autotrophs, Glaucophyta, Rhodophyta, and Viridiplantae (= land plants plus green algae) (see Marin et al. (2005) for an alternative primary endosymbiosis). Subsequently, secondary endosymbioses occurred between green or red algae and heterotrophic eukaryotic hosts. Two algal divisions (Euglenophyta and Chlorarachniophyta) acquired the plastids of green algae, while four algal divisions (Heterokontophyta, Haptophyta, Cryptophyta, and Dinophyta) and one parasitic phylum (Apicomplexa) acquired those of red algae (although some Dinophyta lost their original plastid and remained colorless or re-acquired different plastids as discussed below). An estimated two-thirds of today's algal diversity resulted from secondary endosymbioses (Falkowski et al. 2004; Graham and Wilcox 2000), and thus this process is important in understanding the evolutionary process of plant and algal diversification.

The transition of a symbiont to a plastid involves a series of changes in both the host and the symbiont (Cavalier-Smith 2003; Hashimoto 2005; van der Giezen et al. 2003), which include the establishment of a specific partner alga, lateral gene transfer from the symbiont to the host's nucleus (Katz 2002), the development of protein-transport machinery to carry proteins from the host cytoplasm to the symbiont (van Dooren et al. 2001), and synchronization of cell cycles so that the symbiont can be passed to host daughter cells during host cell division.

Evidence about plastid integration is accumulating (Andersson and Roger 2002; Archibald et al. 2003; Hackett et al. 2004b; Huang et al. 2003; Martin and Herrmann 1998; Martin et al. 2002; Martin 2003a, b; Nozaki et al. 2004; Stegemann et al. 2003), however, the intermediate steps in this process remain largely unknown. Some organisms appear to be in an intermediate stage of plastid acquisition, the best-known examples of which are the Cryptophyta and Chlorarachniophyta, whose plastids contain a vestige of the symbiont nucleus termed a nucleomorph (e.g. Douglas et al. 2001; Gilson et al., 2006). They are thought to represent a late stage of integration. Early stages of plastid acquisition can be found in the dinoflagellates (for reviews, Hackett et al. 2004a; Morden and Sherwood 2002; Schnepf and Elbrächter 1999), where the most dramatic changes are ongoing. The original plastids of dinoflagellates have been of red algal origin, though some dinoflagellates subsequently lost their original red-algal plastids, which were replaced by new ones via extra secondary or tertiary endosymbioses. These examples probably reflect stepwise changes in symbiotic conditions during integration (e.g. Hackett et al. 2004a), and are useful to understand the plastid acquisition process.

We discovered an undescribed flagellate, *Hatena arenicola* gen. et sp. nov., in October 2000, in an intertidal sandy beach in Japan. The organism appears to be in the process of plastid acquisition. Most cells of *H. arenicola* in the natural population have a green plastid-like structure with a red eyespot at the cell apex, though it is inherited by only one of the daughter cells during cytokinesis (Okamoto and Inouye 2005a). Molecular phylogenetic analysis of small subunit ribosomal DNA (SSU rDNA) and ultrastructural observations of the plastid-like structure reveal that it is not a plastid but an autotrophic endosymbiont belonging to the genus *Nephroselmis* Stein (Prasinophyceae, Viridiplantae). We previously reported the symbiotic nature of this association (Okamoto and Inouye 2005a). This paper describes the organism as a new genus and species of katablepharid, a group of flagellates recently designated the phylum Kathablepharida, division Katablepharidophyta (Okamoto and Inouye 2005b). We compare the symbiosis of *H. arenicola* with other examples of secondary symbioses in dinoflagellates to help elucidate the intermediate steps in the plastid acquisition process.

Results

Description

Hatena arenicola Okamoto et Inouye gen. et sp. nov.

Latin Diagnosis

Cellulae oblongae secus axem dorsiventrem valde appresae, sine chromatophoro nec vacuola contractili; 30-40 μm longae; 15-20 μm latae; ventraliter subapicali cum sulco vadoso longitudinali 3-4 μm longa et ca. 2 μm lata; flagellis crassis binis inaequalibus in sulco insertis; flagello anteriore longiore, altero posteriore breviore; ejectisomis conspicuis distichis prope flagellas longitudinaliter positis; plerumque cum 1-4 endosymbiontis viridis; uni stigma endosymbionti situm ad apicem cellulae.

Holotype: Figure 1A

Type locality: Isonoura, Wakayama, Japan (Fig. 1 B-C)

Etymology:

Hatena = 'enigmatic' in Japanese
arenicola = 'inhabiting sand' in Latin

Light Microscopy

General Morphology: The cell is flattened along the dorsiventral axis. In the ventral view, it is ovoid, 30-40 μm long and 15-20 μm wide (Fig. 1 A, D-F). The cell has a furrow in the subapical region, 3-4 μm long and ca. 2 μm wide (Fig. 1 D). The long anterior flagellum and shorter posterior flagellum emerge from this furrow, and two rows of ejectisomes are easily visible near the posterior end of the furrow (Fig. 1 D). One large nucleus is located in the middle posterior region of the cell, and the rest of the cytoplasm is mostly occupied by the plastid of the green symbiont. Cells only rarely lacked the symbiont (Fig. 1 E), though some symbionts were not fully developed (Fig. 1 F; see Discussion).

Cell Division: During cell division, one daughter cell inherits the *Nephroselmis* symbiont while the other does not and becomes colorless. Figure 1 G-L shows cell division in *H. arenicola* (ventral view). First, the host nucleus moves to the apex between the flagellar insertion and the eyespot (Fig. 1 G). The symbiont contracts to the left side of the host cell (on the viewer's right in figures) so that the left half of the cell remains green, while the right half becomes colorless (Fig. 1 G). Two new flagella are formed, and one set moves from the right side of the nucleus to the left (flagellar transformation;

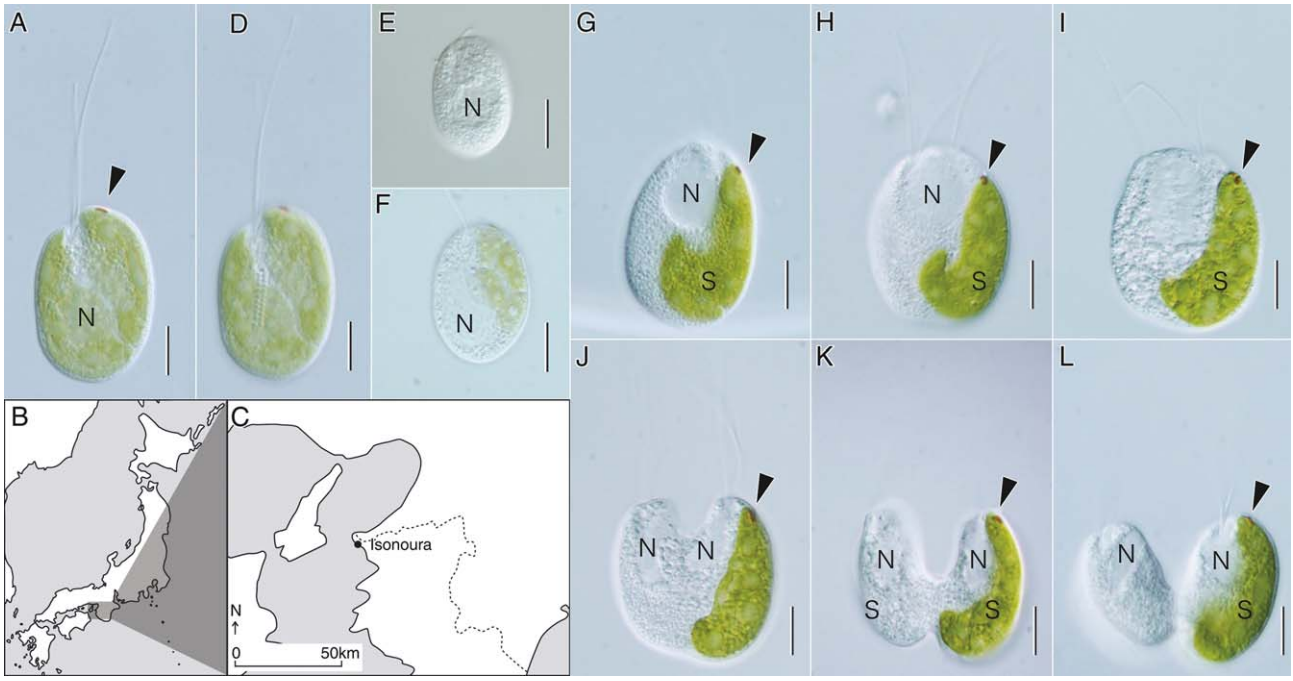

Figure 1. *Hatena arenicola* gen. et sp. nov. **A.** Ventral view of a symbiont-bearing cell showing two flagella and an eyespot of the symbiont (arrowhead). **B,C.** Sampling site. **D.** The same cell in a different focal plane, showing two rows of conspicuous Type I ejectisomes. **E.** A cell lacking the symbiont. **F.** A cell with an "immature" symbiont. **G-L.** Cell division in *Hatena arenicola*, where the arrowhead indicates an eyespot of the symbiont. Each panel shows a different individual at a different stage in cell division. **N:** nucleus. **S:** Symbiont. The scale bar is 10 μm in **A, D-L**.

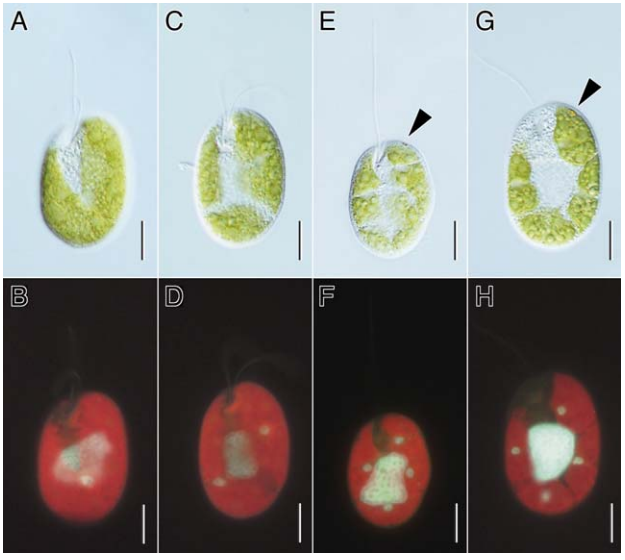

Figure 2. *Hatena arenicola* and its symbiont. DIC images are shown in upper column (**A, C, E, G**) and the fluorescent images of the same cells are shown in lower column (**B, D, F, H** respectively). Arrowheads indicate the eyespot. Blue: DAPI-stained nuclei of *Hatena arenicola* (large fluorescence in the center of the cell) and of the symbiont (smaller dots). Red: Autofluorescence of the symbiont plastid. The scale bar is 10 μm.

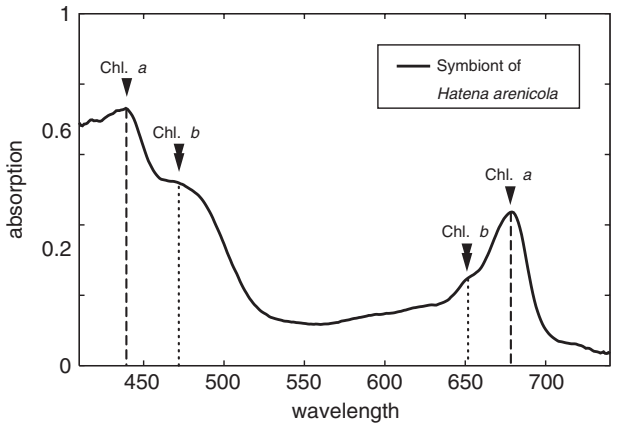

Figure 3. Microspectrophotometry of the symbiont plastid. Spectrogram shows absorbance similar to chlorophyll *a*/*b*-containing plastids.

Fig. 1 H). The chromosomes separate (Fig. 1 I). Following nuclear division (Fig. 1 J), cytokinesis results in one green cell with the symbiont and one colorless cell without it (Fig. 1 K-L).

Fluorescence Microscopy: Figure 2 A-H shows DIC and fluorescence images of the same cells. DAPI label (blue) indicates a large host nucleus in the cell center and one to four smaller symbiont nuclei (Fig. 2 B,D,F,H). Each symbiont nucleus is independent of all others and is surrounded by plastid(s), shown in red (due to autofluorescence). Interestingly, the cell with multiple symbiont nuclei has only a single eyespot at the apex of the host cell (Fig. 2 E-G; arrowheads).

Microphotometry: Microphotometry of seven cells shows an absorption pattern characteristic of plastids with chlorophyll *a*/*b*. Average absorption is shown in Figure 3. The prominent peaks at 435 and 678 nm represent chlorophyll *a* absorption, while the smaller peaks at 470 and 650 nm correspond to chlorophyll *b* absorption.

Uptake of Prey Cells and Symbiont Specificity: Molecular phylogenetic analysis of 16S rDNA indicates that the symbiont is a member of *Nephroselmis* (Okamoto and Inouye 2005a). In feeding experiments using a *Nephroselmis* strain (NIES1417; different from that of the symbiont in 16S rDNA sequence; data not shown), colorless cells of *H. arenicola* phagocytotically engulfed the alga (Fig. 4 A-I) and tentatively maintained it. However, none developed fully, likely because the strain used in the experiments was not the exact symbiont of *H. arenicola*. This suggests that symbiont specificity is at the species or strain level. As the *H. arenicola* cells which engulfed *Nephroselmis* NIES1417 died, it is unclear whether the *Nephroselmis* cells were digested.

Crawling Motion: *Hatena arenicola* displays a conspicuous crawling motion that makes it easy to recognize this organism in a crude sample. Figure 5 A-H illustrates cell motion and flagellar movement. The anterior flagellum produces most of the propulsion, while the posterior flagellum is used to change direction. To move forward, a cell casts the anterior flagellum, which adheres to the substratum by its tip (Fig. 5 A-C), and pulls itself forward (Fig. 5 D, E). It then anchors itself with the posterior flagellum (Fig. 5 F-H), and repeats the process. The tip of the flagellum is sharply bent while it is attached to the substratum, as shown in the supplemental material and in Figure 5 I. The cell bends the posterior flagellum to change direction (not shown).

Electron Microscopy

Electron microscopy (EM) revealed that the green plastid-like structure in the cell is a eukaryotic

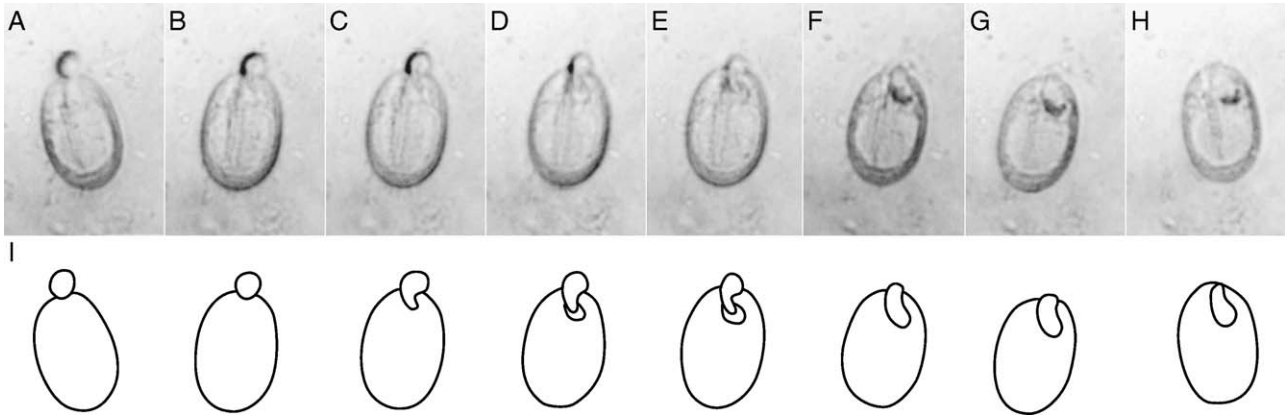

Figure 4. Uptake of *Nephroselmis* (NIES1417) by *Hatena arenicola*. **A-H** were taken at 6-s intervals. **I:** corresponds to *Hatena arenicola* and the symbiont of each frame.

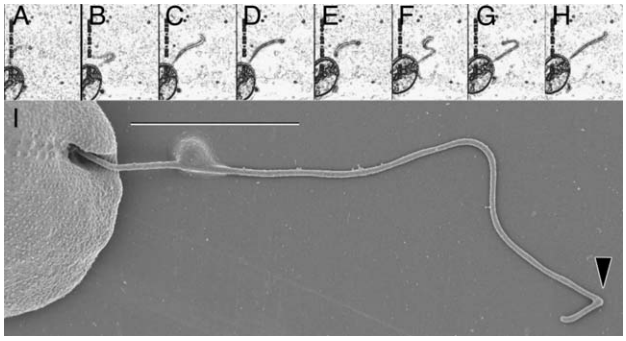

Figure 5. Crawling motion of *Hatena arenicola*. High-speed video images recorded at 0 ms (**A**), 60 ms (**B**), 100 ms (**C**), 130 ms (**D**), 220 ms (**E**), 280 ms (**F**), 300 ms (**G**), 340 ms (**H**), respectively. **I.** SEM image showing the anterior flagellum sharply bent at the distal end (arrowhead). The scale bar is 10 μm in **I**.

endosymbiont. A single nucleus, usually dorsiventrally flattened, is located in the middle posterior region of the cell, and its chromatin is always condensed and electron dense (Fig. 6 A,B). Multiple mitochondrial profiles are present throughout the cytoplasm, though these could be different sections of a single, large reticulate mitochondrion. Mitochondrial cristae are tubular (Fig. 6 C), and there is a single large Golgi body near the groove of flagellar insertion between the nucleus and the flagellar apparatus (Fig. 6 D).

Ejectisomes: There are two types of ejectisomes beneath the membrane: large, Type I ejectisomes sensu Vørs 1992b (Fig. 6 D-E) that are arrayed in two rows near the flagellar insertion (Figs 1 D, 6 F-G); and smaller Type II ejectisomes sensu Vørs 1992b (Fig. 6 H-I) that are arrayed in numerous rows all over the cell (Fig. 6 F-G). Each ejectisome consists of a coiled ribbon with a gradual depression (Fig. 6 D, H), and bound by a single membrane. Discharged ribbons are slightly curved (Fig. 6 J; type I ejectisome). The ribbon does not have any kink, unlike those of Cryptophyta.

Type II ejectisomes are situated beneath the plasma membrane of the cell (Fig. 7 A,B) except for a small smooth area in the apical region, below which the eyespot is situated (asterisk in Fig. 6 G). The ejectisomes are spaced regularly between longitudinally oriented cytoskeletal microtubular bundles (arrowheads in Fig. 7 A).

Hatena arenicola lacks Type III ejectisomes that are characteristic of the genus *Leucocryptos* (Vørs 1992b).

Cellular and Flagellar Covering: The plasma membrane of each cell has a characteristic cellular covering composed of a thick inner basal layer (asterisk in Fig. 7 B) and an outer layer of electron-opaque material (arrowhead in Fig. 7 B). This structure extends to the flagellar surface. The outer layer comprises a regularly arrayed and spiraling envelope around the whole flagellum (Fig. 7 C).

Endoplasmic Reticulum: The endoplasmic reticulum (ER) does not form a conspicuous stack but is loosely distributed throughout the cell. The rough ER extends beneath the surface of the cell (double arrow in Fig. 7 B).

Flagella and Basal Bodies: The long anterior and shorter posterior flagella emerge from a

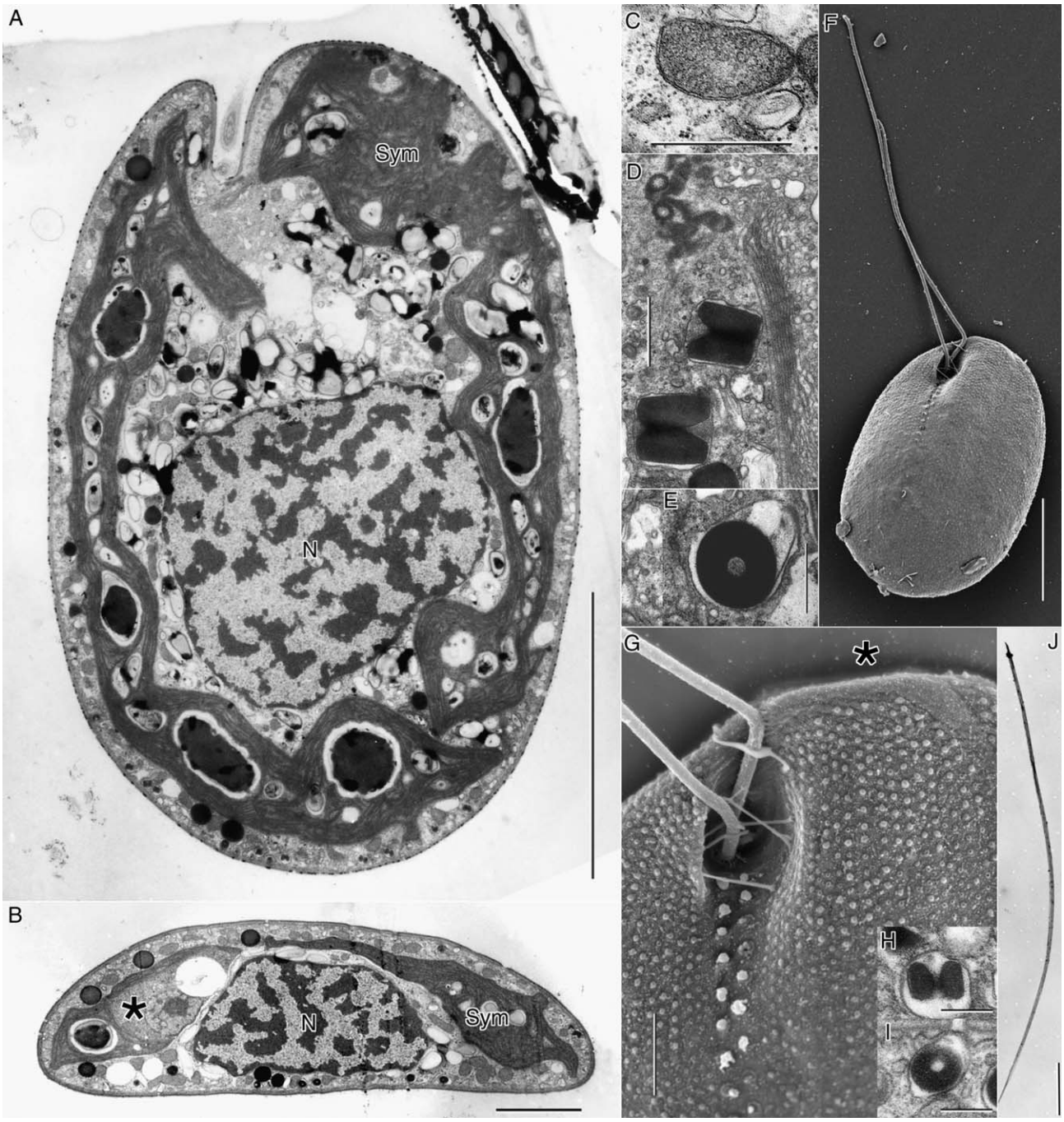

Figure 6. Ultrastructure of *Hatena arenicola*. **A.** A longitudinal section of a *Hatena arenicola* cell showing a nucleus (N). Most of the nuclear content is condensed. The rest of the cytoplasm is occupied by the symbiont (Sym). The symbiont has a large plastid region with multiple pyrenoids. **B.** A transverse section of *Hatena arenicola* showing host nucleus (N) and the symbiont (Sym) with the vestigial cytoplasm (asterisk). **C.** Mitochondrial profiles showing tubular cristae. **D.** A Golgi body near the flagellar basal bodies (arrows) and Type I ejectisomes sensu Vørs 1992 (nearly longitudinal view). **E.** A transverse section of a Type I ejectisome (sensu Vørs 1992). **F.** SEM image of *Hatena arenicola* showing Type I ejectisomes near the flagellar insertion as well as smaller ejectisomes (Type II ejectisomes sensu Vørs 1992) regularly arrayed over the cell surface. **G.** Magnified SEM image of the same cell. Note that the apical region of the cell (asterisk) lacks ejectisomes. **H.** A longitudinal section of Type II ejectisome. **I.** A transverse section of Type II ejectisome. **J.** A whole mount TEM image of a discharged type I ejectisome. The scale bar is 10 μm in **A, E**; 2 μm in **B, G**; 50 nm in **C**; 500 nm in **D, F**; 1 μm in **I**; 200 nm in **H, I**.

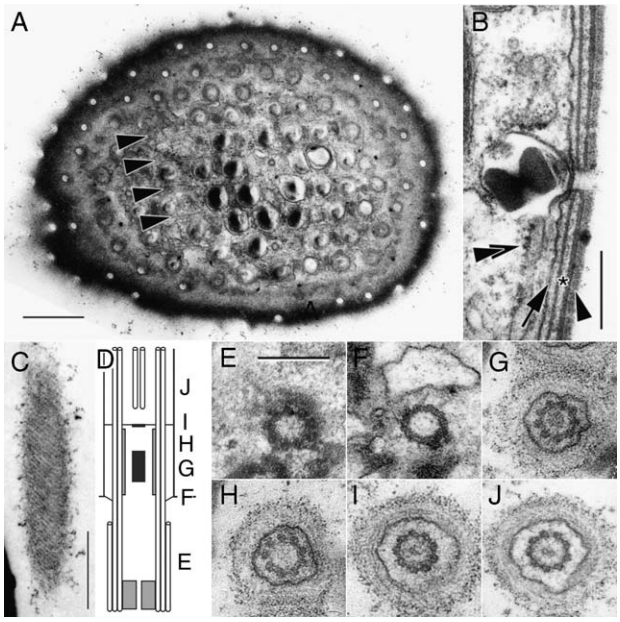

Figure 7. Surface structure and flagellar transition region of *Hatena arenicola*. **A.** A tangential section of the surface of *Hatena arenicola*. Cytoskeletal microtubular bundles (arrows) are arrayed longitudinally below the cell surface; Type II ejectisomes are situated between them. Each pore corresponds to the position of an ejectisome, where the surface sheath is thin. **B.** A transverse section of the cell periphery showing a bilayered surface sheath. An arrowhead indicates the outer layer. An asterisk indicates the thick basal layer. An arrow indicates the plasma membrane. A double arrowhead indicates a profile of rough ER. **C.** A tangential section of the flagellum shows the outer layer of the surface sheath enveloping the flagellum in a spiraling fashion. **D-J.** Flagellar transition region of *Hatena arenicola*. **D.** Diagram of flagellar transition region reconstructed based on serial ultrathin sections. Each letter in **D** indicates which part corresponds to one of the transverse sections (**E-J**). The scale bar is 500 nm in **A, C**; 200 nm in **B, E-J**.

shallow subapical furrow. The flagella are coated by a "surface sheath". The diagram of the basal body and the flagellar transition zone (Fig. 7 D) is based on serial sections of the flagellar transition zone (Fig. 7 E-J). At the proximal end of the basal body, there is a cartwheel structure with a central tube. The triplet microtubules of the basal body terminate below the plasma membrane (Fig. 7 E), whereas the doublet microtubules attach to the plasma membrane by a connecting fiber (Fig. 7 F). The flagellar transition region extends above the plasma membrane, and an electron-dense rod structure is present (Fig. 7 G) in the middle of this region. Surrounding the transition region are outer doublet microtubules lined in a loose, electron-dense material (Fig. 7 H). The flagellar transition region ends in a terminal plate with electron-opaque material at the center (Fig. 7 I). The axonemal central pair begins above the terminal plate (Fig. 7 J).

Feeding Apparatus: As reported in Okamoto and Inouye (2005a), colorless cells lacking the symbiont have a complex feeding apparatus at their apex (Fig. 8 A-C), consisting of transverse tubular rings (arrowheads in Fig. 8 B-C) and longitudinal microtubules arrayed in a single layer (arrow in Fig. 8 B-C). These microtubules are different from those that form the cytoskeleton (double arrowheads in Fig. 8 A). Inside the microtubular skeletons of the feeding apparatus are several electron-opaque granules, some of which are large and elongate (light gray) and others that are smaller, granulated, and pigmented (Fig. 8 A, C). These granules are restricted to the feeding apparatus, never seen elsewhere in the cell. Symbiont-bearing cells do not have a feeding structure; the corresponding region is occupied by the eyespot of the symbiont (Fig. 8 D-E).

Symbiont: The symbionht retains not only a plastid but also its own cytoplasm with a nucleus and mitochondrion(a) (Fig. 9 A-C). Most symbiont cells contain one nucleus, which is often attached to the membrane, and symbiont and host nuclei often face each other (Fig. 9 A-C). The symbiont is bounded by a single membrane (**arrowhead in Fig. 9 D**), whose origin is unknown. Mitochondria have flat, often degraded cristae, though the extent of degradation varies among individual cells (Fig. 9 E-F). The plastid, which is the largest structure in the symbiont (Fig. 6 A-B), contains multiple pyrenoids bounded by a thin starch sheath (Fig. 9 G). The pyrenoid has shallow invaginations of the thylakoid membrane. The plastid has a single conspicuous eyespot, where the morphological association between host and symbiont is present (see below).

Free ribosomes are densely distributed throughout the symbiont cytoplasm, though no ribosome-bearing membrane (rough ER) is present. Occasionally there are flattened, stacked membranes next to the nucleus (Fig. 9 A). This structure would normally be a Golgi body but it is present in a degraded or inactive form, because no Golgi vesicles were seen around the structure. Some randomly shaped vacuoles of unknown origin are also present (Fig. 9 B-C). Because each cell division will result in half the population carrying

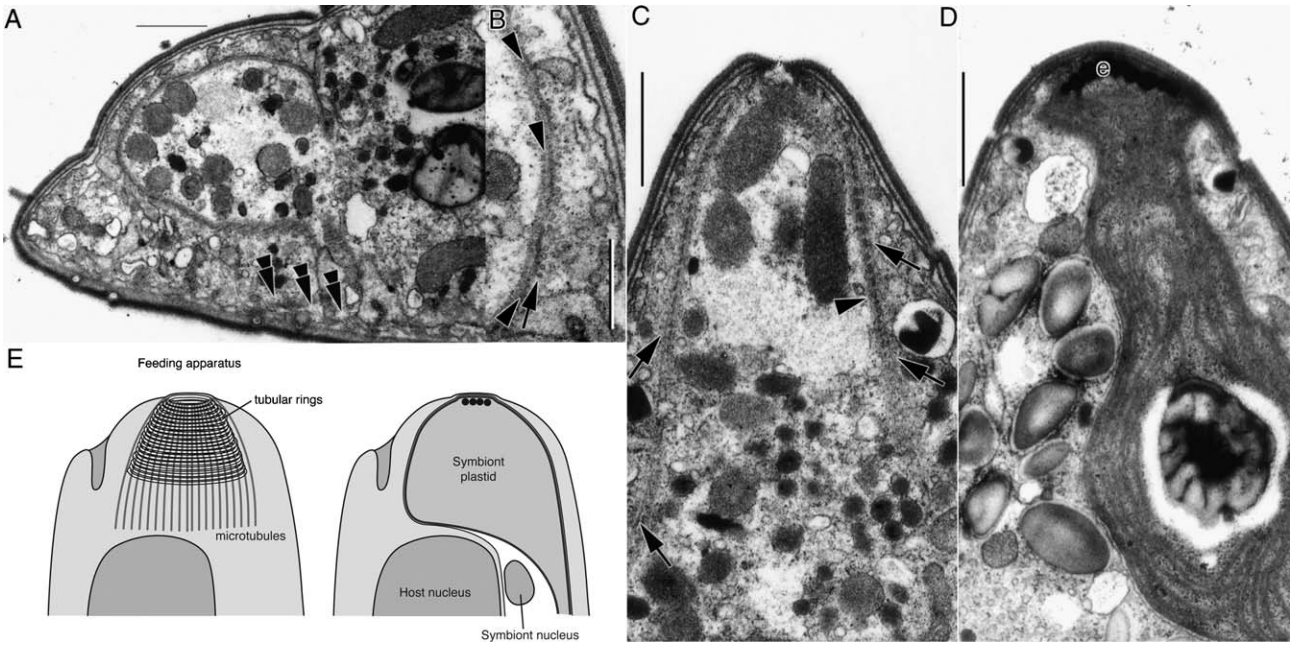

Figure 8. Feeding apparatus of *Hatena arenicola*. **A.** A nearly transverse section of the feeding apparatus. Feeding apparatus is distinct from cytoskeletal microtubules (double arrowheads). **B.** A magnified view showing microtubules (arrow) regularly arrayed in a single layer along the external side of the tubular rings (arrowheads). **C.** Longitudinal section of the feeding apparatus showing numerous transverse tubular rings (arrowhead) and longitudinal microtubules arrayed in a single layer (arrows). **D.** An eyespot (e) of symbiont is located at the corresponding place in the symbiont bearing cell. **E.** A schematic illustration of the feeding apparatus and the corresponding place of the symbiont-bearing *Hatena arenicola*. The scale bar is 500 nm in **A, C**-**D**; 250 nm in **B**.

the symbiont, these morphological varieties likely reflect degradation (see Discussion).

Cytoskeletal structures, including the flagella, basal bodies, the flagellar apparatus, and microtubular rootlets, are completely absent. These morphological changes must affect intracellular functions, such as protein synthesis and distribution in the symbiont (see Discussion).

The lysosome of the host cytosol is discontinuous with the symbiont compartment. The lysosome of some cells contains scales of *Nephroselmis* and *Pyramimonas* (Fig. 10 A,B), indicating that *H. arenicola* cells engulf other prey in addition to its *Nephroselmis* partner. Because *Pyramimonas* cells are digested, *H. arenicola* may be partly heterotrophic (see Discussion).

Eyespot: The eyespot is composed of a single-layered sheet of osmiophilic granules (Fig. 11 A) that connects to the inner plastid envelope. Near the eyespot, the plastid, symbiont, and host plasma membranes are tightly layered (Fig. 11 A,B). In some cells, single microtubules are aligned longitudinally between the plasma membrane and the symbiont membrane overlying the eyespot region (Mts in Fig. 11 C,D). These single microtubules are distinct from the cytoskeletal microtubular bundles (arrowhead in Fig. 11 D), and the space between them lacks Type II ejectisomes; this is consistent with the smooth surface appearance of the eyespot region (Fig. 6 F).

Molecular Phylogeny

Partial SSU rDNA sequences of *H. arenicola* (AB212285) aligned with the homologues of known eukaryotes were subjected to phylogenetic analyses. The resulting maximum likelihood (ML) tree (Fig. 12) showed the typical topology of the SSU rDNA tree, and *H. arenicola* was included in the katablepharid clade, which was robustly supported with high bootstrap probability in ML (99%), NJ (100%), and MP (99%) analyses.

Discussion

Hatena arenicola has several unique features that suggest it is in the process of endosymbiosis with

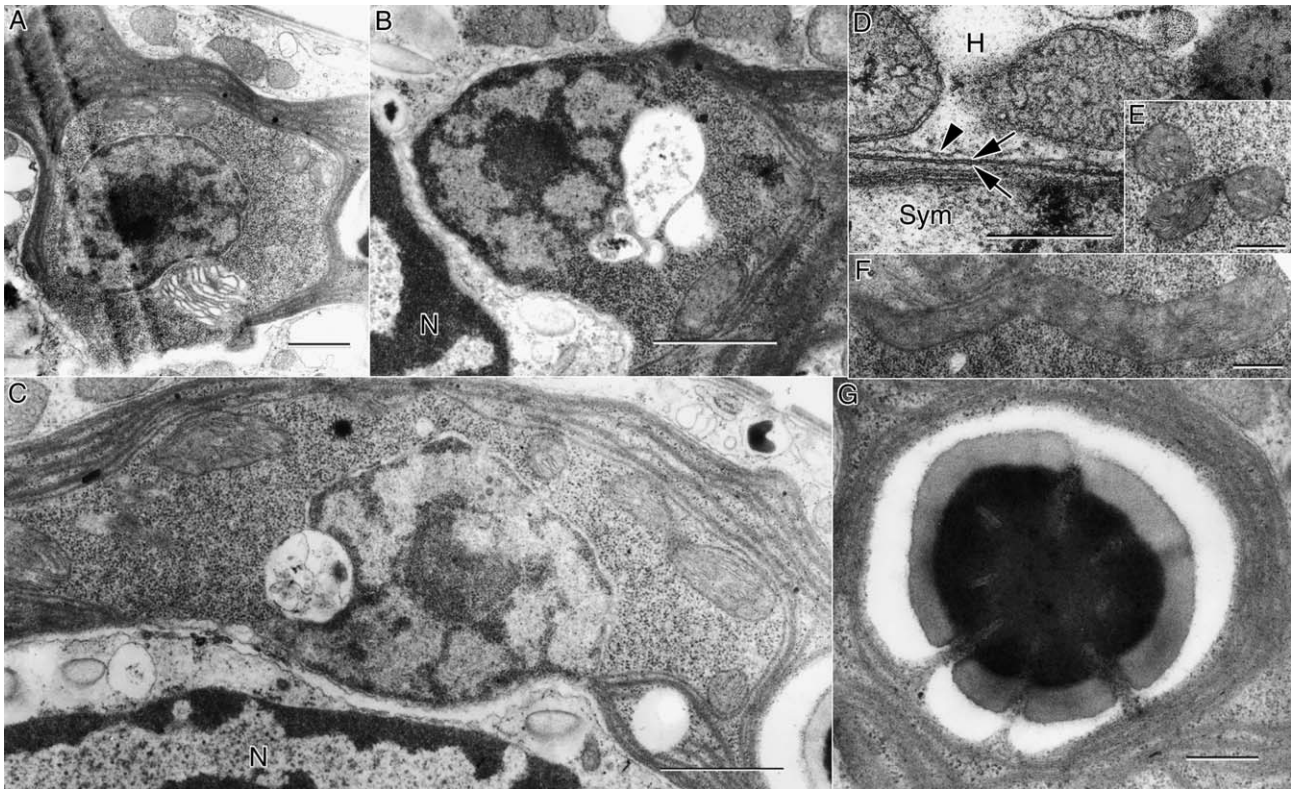

Figure 9. Ultrastructure of the symbiont. **A-C.** The symbiont cytoplasm, retaining a nucleus, mitochondria, and sometimes a Golgi body-like vesicle **(A)** or membranes of random shape (**B-C**), likely in an intermediate state of integration. **D.** The single symbiont-enveloping membrane (arrowhead) separates the symbiont compartment (Sym) and host cytoplasm (H). Double membranes of the symbiont plastid are also shown (arrows). **E.** Mitochondrial profiles that retain flat cristae. **F.** A relatively degenerated mitochondrial profile. **G.** A pyrenoid, surrounded by a starch sheath. Random shallow invagination of the thylakoids. The scale bar is 1 μm in **A-C**; 250 nm in **D-G**.

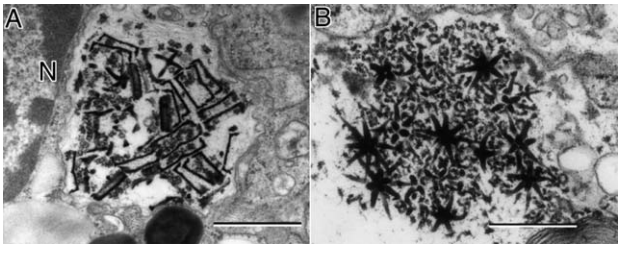

Figure 10. Lysosome of *Hatena arenicola* with scales of prasinophytes characteristic to *Pyramimonas* (**A**) and *Nephroselmis* (**B**) respectively. The scale bar is 500 nm.

a *Nephroselmis* partner (Okamoto and Inouye 2005a). We will discuss the taxonomy and classification of *H. arenicola* first, and then focus on its unique endosymbiosis.

Taxonomy

Morphological and molecular analyses of *H. arenicola* clearly show that it belongs to the recently established division/phylum Katablepharidophyta (International Code of Botanical Nomenclature, ICBN)/Kathablepharida (International Code of Zoological Nomenclature, ICZN) (Okamoto and Inouye 2005b). The katablepharids comprise an ultrastructurally well-defined and small group of heterotrophic flagellates that includes 10 species in two genera: nine species of *Katablepharis* Skuja (correct spelling in ICBN which will be used in this paper)/*Kathablepharis* Skuja (original spelling in the ICZN), and one species of *Leucocryptos* (Braarud) Butcher. Katablepharidaceae (ICBN) was originally described by Skuja (1939) based on ovate or cylindrically ovate cell shape, two flagella emerging from a subapical depression, and conspicuous ejectisomes aligned

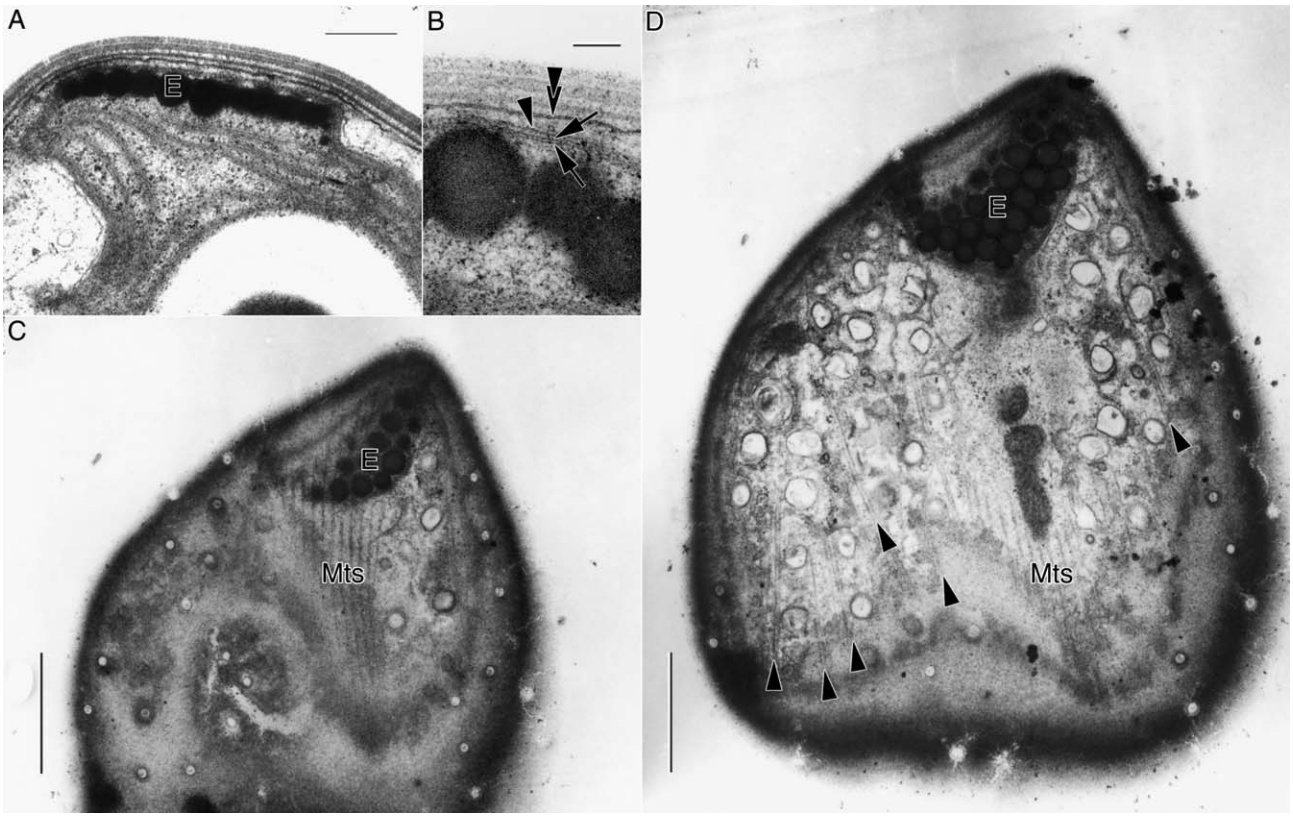

Figure 11. Eyespot of the symbiont plastid. **A.** A longitudinal section of the eyespot (E). **B.** A magnified view of another cell clearly shows the eyespot granules, the inner/outer envelop of the symbiont plastid (arrows), the single symbiont enveloping membrane (arrowhead), and the host plasma membrane (double arrowhead) associated with each other. **C-D.** Tangential sections of the eyespot region show single microtubules (Mts) distinctive from the cytoskeletal microtubules (arrowheads) longitudinally situated between the eyespot (E) and the plasma membrane. The scale bar is 250 nm in **A**; 100 nm in **B**; 1 μm in **C-D**.

in two rows near the flagellar insertion. Vørs (1992b), and Clay and Kugrens (1999b) emended the family by adding the following ultrastructural features: the entire surface of the cell, including the flagella, is coated with a bilayered surface sheath that appears to form spiraling rows around the cell body; tubular mitochondrial cristae; a complex, truncated conical feeding apparatus and cytoskeleton; a Golgi apparatus situated anteriorly and a centrally located nucleus; and a food vacuole in the posterior part of the cell.

Hatena arenicola shares all these characters, except that the cell is dorsiventrally compressed and the food vacuole is absent. We occasionally observed a vacuole containing scales of prasinophytes, though its position was anterior to the nucleus. In addition, the flagellar transition zone containing a rod-shaped structure is fundamentally the same as that of *K. ovalis* (Lee et al. 1992). Based on these ultrastructural similarities and the molecular phylogenetic data, *H. arenicola* undoubtedly belongs to the katablepharids.

Currently, all the katablepharids belong to a single family, Katablepharidaceae, whose cells are defined as either "oblong or cylindrically ovate" (*Katablepharis*; Clay and Kugrens, 1999b; Vørs, 1992b) or "ovate, pyriform elliptical outline" (*Leucocryptos*; Butcher 1967). The most important distinguishing feature of *Leucocryptos* is the presence of Type III ejectisomes, which have been found only in *Leucocryptos*. Because *H. arenicola* lacks Type III ejectisomes, it does not belong to *Leucocryptos*.

Hatena arenicola is distinct from all other katablepharids previously described in that it is dorsiventrally compressed with a flat-oval shape, which suggests that it does not belong to the genus *Katablepharis*. Its crawling motion and the feeding apparatus composed of single-layered microtubules are also distinctive from the other

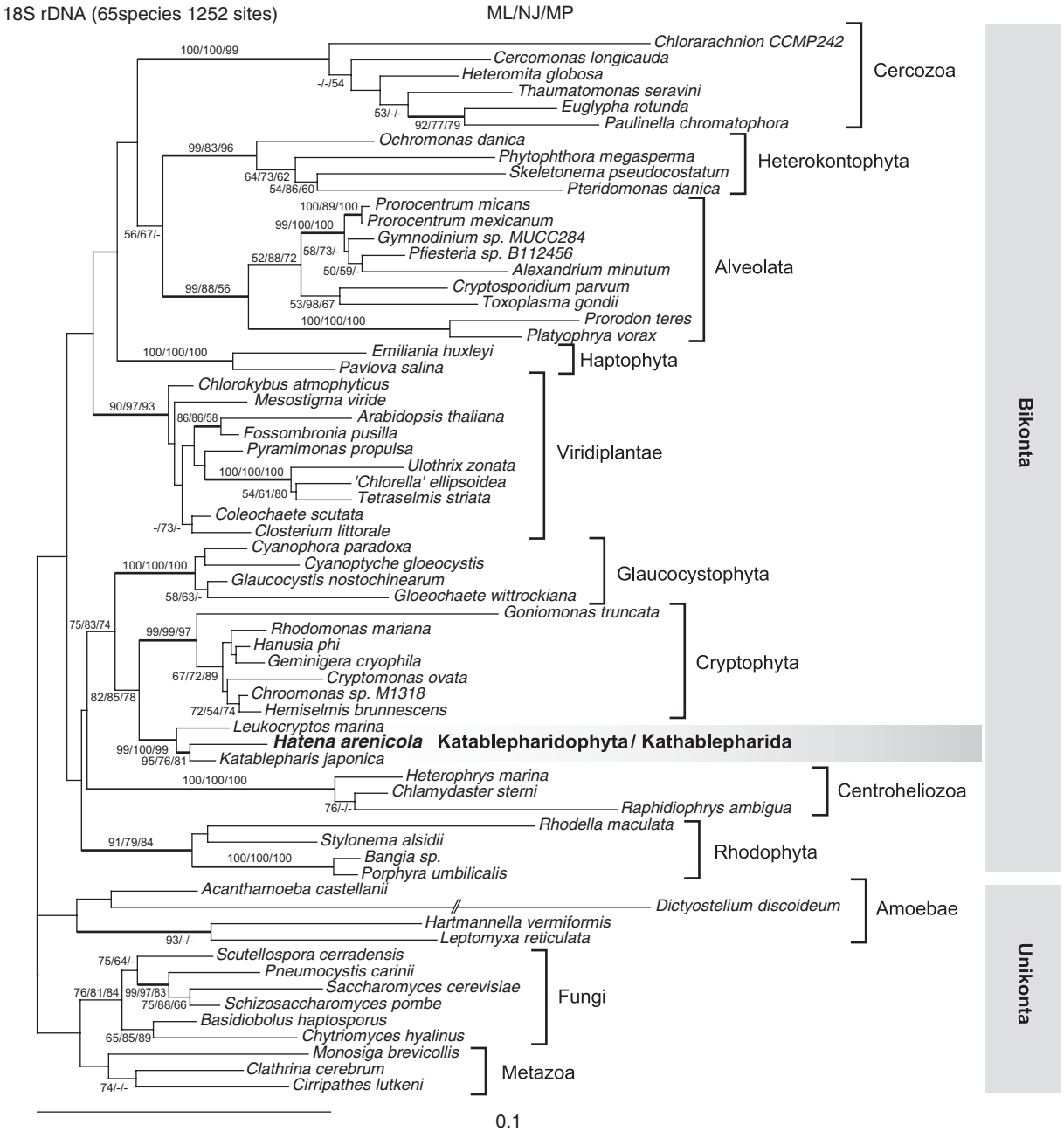

Figure 12. Unrooted eukaryotic tree based on the SSU rDNA. The best tree of the ML method is shown. Bootstrap propotions are shown at the internal branches, in the order of ML/NJ/MP methods. The length of each branch is proportional to the estimated number of substitutions. Bar denotes 10% substitutions per site. For details of the phylogenetic reconstruction methods, see text. The organisms included in the tree are listed in Table 1. Unambiguously aligned 1252 nucleotide positions were used for the analysis.

katablepharids (Clay and Kugrens 1999a, b; Kugrens et al. 1994; Lee and Kugrens 1992; Lee et al. 1991; Okamoto and Inouye 2005b; Vørs 1992a, b). Based on those features, we propose that the organism should be assigned to a new genus, *Hatena*.

The family-level taxonomy of the katablepharids is still unclear, primarily because little molecular sequence data exist. Until further studies elucidate katablepharid taxonomy, it is best to include the genus *Hatena* in the family Katablepharidaceae.

Endosymbiosis

Endosymbiosis is a major driving force in plant evolution, and thus it is important to understand this process. *Hatena arenicola* may be an important model of early plastid acquisition. Symbiotic *Nephroselmis* differs from free-living individuals in having enlarged plastids with a greater number of pyrenoids, degraded subcellular structures, and morphologically distinct eyespots. Cells of known *Nephroselmis* species are a maximum of 20 μm in length (*Nephroselmis astigmatica*; Inouye and Pienaar 1984) and possess a single plastid with a single pyrenoid. The symbiont occupies most of the host cytoplasm, suggesting that the symbiont plastid(s) grows more than ten fold after being engulfed by the host. Pyrenoids also multiply after being engulfed. In contrast, the symbiont cytoplasm loses other major cell components including flagellar apparatus and microtubular roots, endomembranes such as the ER and transport vesicles, Golgi-like vesicles, and amorphous membranous structures. The dramatic growth of the plastid is in stark contrast to the degradation of the other organelles. Because the cytoplasm is in such a degraded state, it must be difficult to sustain the growth and maintenance of the plastid alone. It is likely that some metabolites from the host cell are used to develop and maintain the plastid.

Eyespot Morphology

The morphology of the eyespot is most suggestive of a host-symbiont coordination. The tight layering of the four distinct membranes of different origin implies functional cooperation. The eyespot is an important component of a photo-sensing complex found in various algal groups (Melkonian and Robenek 1984; Gualtieri 2001). It effectively regulates the light received by a photoreceptor located on a nearby membrane, thereby allowing the alga to detect light direction. Preliminary observations have shown that lateral, and not vertical, incidence, is important for the behavior of *H. arenicola*. Hence, we speculate that the photoreceptor and the regulatory mechanism would be laterally aligned in the cell, so that the eyespot can effectively shade the photorecepter from the lateral incidence. Assuming that the eyespot is functional in *H. arenicola*, the photoreceptor should be situated in either of the outer or inner plastid membrane, the single endosymbiont envelope, or the plasma membrane. Their morphological association can be explained as a consequence of functional collaboration. Because *H. arenicola* crawls two-dimensionally, a phototactic response to laterally projected light is plausible. To test whether a functional association exists, further investigation of the threshold and the efficiency of phototaxis in both colored and colorless *H. arenicola* cells are required.

Morphological Changes of the Host and "Half-plant, half-predator" Model

Hatena arenicola cells without a symbiont have a complex feeding apparatus in place of an eyespot, indicating that symbiont acquisition is accompanied by drastic morphological changes in both the symbiont and the host.

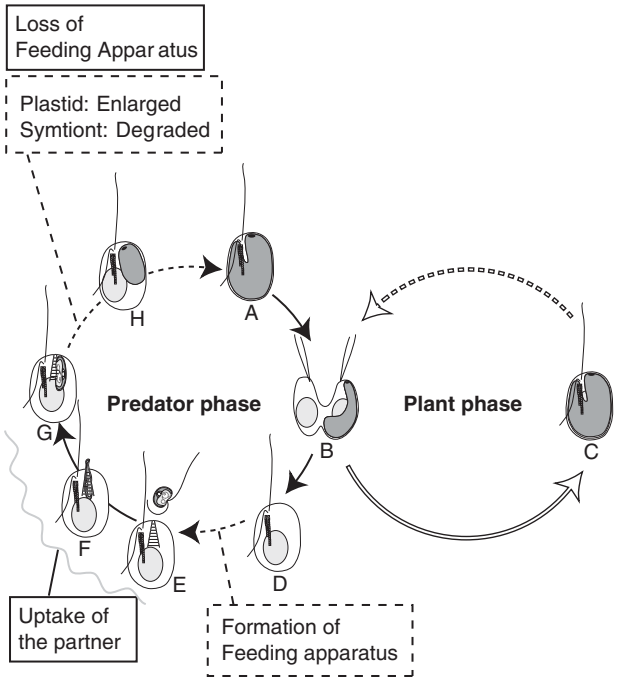

Figure 13. Half-plant, half-predator-hypothesis. The solid line indicates a witnessed process, and the broken line indicates a hypothetical process. **A-D:** A green cell with the symbiont, lacking the feeding apparatus (**A**) divides (**B**) into one green (**C**) and one colorless cell (**D**). **E-G:** The colorless cell should form a feeding apparatus de novo and engulfs a *Nephroselmis* cell. **G-H:** The symbiont plastid selectively grows in the host cytoplasm. Because cell division of a colorless cell or a cell with an "immature" symbiont (**H**) has never been observed, uptake and the subsequent changes in both host and symbiont apparently occur within one generation.

Such structural changes would necessitate life cycle changes. Based on observations presented in this paper, we propose the "half-plant, half-predator" hypothesis, where *H. arenicola* switches its lifestyle between that of a plant and a predator (Fig. 13; see also Okamoto and Inouye 2005a for detailed explanation). This proposed life cycle is also supported by the observation that the extent of degradation of symbiont mitochondria and membranous structures varies among individual cells. The presence of prasinophyte scales in a *H. arenicola* lysosome suggests that *H. arenicola* lives heterotrophically to some extent, perhaps until it engulfs its symbiotic partner. This represents an intermediate state of trophic alteration. Although there are several assumptions in the model, it promises to lead to new insights and helps elucidate the plastid integration process.

Evolutionary Implications

Extra secondary and tertiary endosymbioses in dinoflagellates may represent evolutionary events that occurred during plastid acquisition (for reviews, see Hackett et al. 2004a; Morden and Sherwood 2002; Schnepf and Elbrächter 1999). The earliest stage is represented by the cryptophyte symbiont, in which only cytoskeletal components are lost, as in *Amphidinium latum* Lebour (Horiguchi and Pienaar 1992), A. *poecilochroum* Larsen (Larsen 1988), and *Gymnodinium acidotum* Nygaard (Fields and Rhodes 1991; Wilcox and Wedemayer 1984). The cell cycles of the host and symbiont are not synchronized, and the host cell must repeatedly capture symbionts. The next stage is represented by the symbiont of diatom origin, in which various subcellular structures are lost, except the nucleus, mitochondrion(a) and plastid, as in *Durinskia baltica* (Levander) Carty et Cox (formerly *Peridinium balticum*; Chesnick and Cox 1987, 1989; Chesnick et al. 1997; Eschbach et al. 1990; Tippit and Pickett-Heaps 1976; Tomas and Cox 1973) and *Kryptoperidinium foliaceum* (Stein) Lindemann (Dodge 1971; Eschbach et al. 1990). At this stage, the symbiont divides synchronously with the host cell (Chesnick and Cox 1987, 1989; Tippit and Pickett-Heaps 1976), so that the association between the host and symbiont becomes permanent, and repeated uptake of the symbiont is no longer necessary. Finally, the symbiont cytoplasm is reduced, as seen in *Lepidodinium viride* (Watanabe et al. 1987; Watanabe et al. 1990), *Gymnodinium chlorophorum* (Elbrächter and Schnepf 1996), both with symbionts of prasinophyte origin, and *Karenia brevis* (Davis) Hansen et Moestrup, *Karenia mikimotoi* (Miyake et Kominami ex Oda) Hansen et Moestrup, *Karlodinium veneficum* (Leadbeater et Dodge) Larsen with symbionts of haptophyte origin (Daugbjerg et al., 2000; Inagaki et al., 2000; Tangen and Björnland, 1981). The symbiont of *Karenia* and *Karlodinium* species has no remnant of cytoplasm, and can therefore be recognized as an integrated plastid. Based on cytoplasm reduction and the lack of cell cycle synchronization, the symbiosis of *H. arenicola* can be placed between the cryptophyte and diatom types of symbiosis mentioned above. Nevertheless, their morphological association suggests an intimate host—symbiont relationship. Previous studies on symbiosis in dinoflagellates have focused on symbiont degradation only. In this study, we demonstrated that major morphological changes also occur in the host, suggesting that plastid acquisition is not merely "enslavement" where the symbiont is degraded, but also a process during which the host itself changes to establish a new association with the symbiont.

The rigid pattern of asymmetrical inheritance of the symbiont is also suggestive of a partly regulated association. The symbiont always comes to the left side of the host cell (ventral view) before the migration of the host nucleus, implying an interaction between the symbiont compartment and the host cytoskeleton. If the symbiont moved to the division plane, and not to one side of the cell, the symbiont would co-segregate, just as in the division of *D. baltica*, where the center-positioned symbiont co-segregates upon host cytokinesis (Tippit and Pickett-Heaps 1976).

Another question is whether the association of *H. arenicola* and the symbiont has developed genetic modification. The process of endosymbiosis is hypothesized to include genetic changes such as lateral gene transfer (LGT) from symbiont to host, coupled with evolution of a protein transport machinery from host to symbiont (e.g. Gilson and McFadden 2002). It is unclear when those changes start and how they integrate. Considering host—symbiont intimacy, *H. arenicola* would have already experienced or may be experiencing some of these changes. Therefore, the study of LGT or of a protein transport machinery in *H. arenicola* would be an interesting topic for future studies.

Recently, Marin et al. (2005) reported another example of primary endosymbiosis in *Paulinella chromatophora* Lauterborn, a freshwater thecate amoeba that bears a cyanobacterium-like

structure. They reported that the symbiosis of *P. chromatophora* is a more recent event than the origin of all other plastids, based on the molecular phylogeny of ribosomal DNA operon sequences. This is consistent with a morphological feature of the symbiont, namely, a peptidoglycan layer that must have originated from the cell wall of an ancestral cyanobacterium.

The symbiotic relationships of *H. arenicola*, *P. chromatophora*, and the dinoflagellates probably represent different intermediate steps in plastid acquisition via primary or secondary endosymbiosis. Continued study and comparison of these groups should provide further insight into plastid evolution.

Concluding Remarks

Hatena arenicola gen. et sp. nov. is likely in the process of plastid acquisition via secondary endosymbiosis. Although it is in an early intermediate stage of acquisition, the two organisms have already established an intimate association in ultrastructure and likely in metabolic function. Based on behavioral and ultrastructural observations, we propose a "half-plant, half-predator" life cycle. Because *H. arenicola* shows an early intermediate state of plastid acquisition, it should provide further insight into plant evolution. This study provides a foundation for future studies on the topic.

Methods

Sampling and temporary maintenance in the laboratory: Because it is not possible to culture *Hatena arenicola* in the laboratory, we used crude samples from the natural habitat. Cells were collected at Isonoura Beach, Wakayama Prefecture, Japan (Fig. 1 B,C), April—December from 2000 to 2004. Samples were maintained in the laboratory at room temperature in f/2 medium, under *ca*. 10 μmol photons $m^{-2} s^{-1}$, and the light—dark cycle was L:D = 5:19 h.

Morphological observations: Light microscopy (LM) and fluorescence microscopy (FM) was conducted using a Leica DMR light microscope (Leica Wetzlar GmbH, Wetzlar) and the LM image was taken with a Keyence VB6010 digital chilled CCD camera (Keyence, Osaka). For FM, 4′,6-Diamidino-2-phenylindole (DAPI) was used to stain the nucleus. The DAPI fluorescence along with the autofluorescence of the plastid were observed using a D filter cube (Leica Wetzlar GmbH, Wetzlar).

Microspectrophotometry was performed by majoring three different regions of the symbiont in each of seven cells. Each absorption spectrum was recorded in the range of 300—800 nm with a light microscope (ECLIPSE, Nikon, Tokyo) equipped with a high-resolution multichannel photodetector (MCPD 7000, Otsuka Eelectronics, Osaka) at Okazaki National Institute for Basic Biology, Japan. The average of the three measurements was considered the representative absorbance of each cell. Because the absorptions obtained were almost uniform across the seven cells, their average is shown.

A unialgal culture of *Nephroselmis* sp. (NIES1417) was established from the same sample site by micropipette isolation and maintained in f/2 medium at 20 °C under ca. 10 μE light intensity, and a light-dark cycle of L:D = 14:10 h. The uptake of *Nephroselmis* sp. (NIES1417) was photographed under a CKX31 inversed light microscope (Olympus, Tokyo) equipped with a COOLPIX 990 digital camera (Nikon, Tokyo) at 6-s intervals.

High-speed video images were recorded at 200 frames per second using an OPTIPHOT microscope (Nikon, Tokyo), equipped with an MHS-200 high-speed video capturing system (Nac Inc., Tokyo). The images were digitized on a Macintosh computer using an NIH imaging program (public domain, developed at the US National Institute of Health; available at http://rsb.info.nih.gov/nih-image/) for analysis of the cellular and flagellar motion.

Preparation for transmission electron microscopy (TEM) and scanning electron microscopy (SEM) was performed as described elsewhere (Moriya et al. 2000; Okamoto and Inouye 2005b). The observations were made with a JEOL 100CXII electron microscope (JEOL, Tokyo) and a JSM-6330 scanning electron microscope (JEOL, Tokyo).

Molecular phylogeny: To avoid contamination of the prey genome, single cells of *Hatena arenicola* were isolated with micropipette into a 0.2-ml PCR tube containing 10 μl of sterilized double distilled water, and immediately frozen at −80 °C for more than 15 min to completely disrupt the cells. The first and the second nested PCR were performed with existing degenerate primer sets (Moriya et al. 2000) using rTaq (TOYOBO, Osaka). Thermal cycling for the first PCR consisted of 33 cycles. Annealing temperatures ranged from 50 to 47 °C (six cycles decreasing

Table 1. Sequences used for the phylogenetic analyses

Organism	Accession number
SSU rDNA	
Katablepharidophyta/Kathablepharida	
Hatena arenicola	AB212285
Katablepharis japonica	AB231617
Leucocryptos marina	AB193602
Metazoa	
Cirripathes lutkeni	AF052902
Clathrina cerebrum	U42452
Monosiga brevicollis	AF084618
Fungi	
Basidiobolus haptosporus	AF113413
Chytriomyces hyalinus	M59758
Pneumocystis carinii	L27658
Saccharomyces cervisiae	V01335
Schizosaccharomyces pombe	Z19578
Scutellospora cerradensis	AB041344
Amoebae	
Acanthamoeba castellanii	M13435
Hartmannella vermiformis	M95168
Leptomyxa reticulata	AF293898
Dictyostelium discoideum	K02641
Cercozoa	
Cercomonas longicauda	AF101052
Chlorarachnion CCMP242	U03479
Euglypha rotunda	X77692
Heteromita globosa	U42447
Paulinella chromatophora	X81811
Thaumatomonas seravini	AF411259
Viridiplantae	
Arabidopsis thaliana	X16077
'Chlorella' ellipsoidea	D13324
Chlorokybus atmophyticus	M95612
Closterium littorale	AF115438
Coleochaete scutata	X68825
Fossombronia pusilla	X78341
Mesostigma viride	AJ250108
Pyramimonas propulsa	AB017123
Tetraselmis striata	X70802
Ulothrix zonata	Z47999
Heterokontophyta	
Ochromonas danica	M32704
Pteridomonas danica	L37204
Skeletonema pseudocostatum	X85394
Phytophthora megasperma	X54265
Alveolata	
Cryptosporidium parvum	X64340
Toxoplasma gondii	X75429
Platyophrya vorax	AF060454
Prorodon teres	X71140
Alexandrium minutum	U27499
Gymnodinium sp. MUCC284	AF022196
Pfiesteria sp. B112456	AF218805
Prorocentrum mexicanum	Y16232
Prorocentrum micans	M14649
Cryptophyta	
Chroomonas sp. M1318	AJ007279
Cryptomonas ovata	AJ421147
Geminigera cryophila	U53124
Hanusia phi	U53126
Hemiselmis brunnescens	AJ007282
Rhodomonas mariana	X81373
Goniomonas truncata	U03072
Glaucophyta	
Cyanophora paradoxa	X68483
Cyanoptyche gloeocystis	AJ007275
Glaucocystis nostochinearum	X70803
Gloeochaete wittrockiana	X81901
Haptophyta	
Emiliania huxleyi	L04957
Pavlova salina	L34669
Rhodophyta	
Bangia sp.	AF043362
Porphyra umbilicalis	AB013179
Rhodella maculata	U21217
Stylonema alsidii	L26204
Centroheliozoa	
Chlamydaster sterni	AF534709
Heterophrys marina	AF534710
Raphidiophrys ambigua	AF534708

the temperature by 0.5 °C for each cycle, and 27 cycles at a constant temperature). An extension was performed at 72 °C for 1 min, and denaturing was done at 94 °C for 30 s. The final extension period was at 72 × C for 7 min. Thermal cycling for the second PCR consisted of 33 cycles with an annealing step at 53 °C for 30 s, an extension step at 72 °C for 1 min, and denaturing at 94 °C for 30 s, with a final extension period at 72 °C for 7 min. The sequences were determined by direct sequencing. Cycle sequencing reaction was performed using a DYEnamic ET terminator cycle sequencing kit (Amersham biosciences, Buckinghamshire), as per the manufacturer's instructions. Sequencing was conducted with an ABI PRISM 377 DNA Sequencer (Applied Biosystems, California), and sequences were confirmed free of contaminants and not of haptophyte prey origin by comparing at least two cells or performing a BLAST search at the National Center for Biotechnology Information (NCBI) server (http://www.ncbi.nlm.nih.gov/

BLAST/). The sequence (AB212285) was deposited to GenBank.

The SSU sequence was manually aligned to the existing alignments of global eukaryotes (Okamoto and Inouye 2005b), which include 65 taxa for SSU rDNA (Table 1). To avoid the long-branch attraction (LBA) artifact in SSU rDNA analysis, organisms with an extraordinary evolutionary rate, such as the Euglenozoa, the diplomonads, and the palabasalids, were excluded after confirming that they are not a sister group of the katablepharids. A total of 1252 unambiguously aligned nucleotide positions were selected for phylogenetic analyses.

The maximum likelihood (ML), neighbor joining (NJ), and maximum parsimony (MP) methods for phylogenetic analysis were applied to the data set using PAUP* ver.4.0 b 10 (Swofford 2003). In the ML analysis, the evolutionary model was selected using the Akaike information criterion (AIC) test in Modeltest ver.3 (Posada and Crandall 1998), which selected the general time reversible (GTR) model with rate variation among sites and invariant sites (GTR+I+gamma). The estimated gamma-shape parameter (alpha) of the discrete gamma-distribution was 0.5645, and the proportion of invariant sites was 0.3257. A further tree search with GTR+I+gamma model with eight site rate categories that approximates site rate was used to produce the optimal tree. Bootstrap proportion (BP) values for internal branches of the optimal tree of the ML analysis were obtained using PAUP* through 300 bootstrap resamplings for the ML method and 1000 resamplings for the NJ and MP methods.

Acknowledgments

We thank Dr. Masakatsu Watanabe and Dr. Shigeru Matsunaga (Graduate University for Advanced Studies, Japan) for their dedication to the microspectrophotometric work and assistance in sampling, and Dr. Hiroshi Kawai (Research Center for Inland Seas, University of Kobe) for use of his laboratory equipment. We appreciate Dr. Tetsuo Hashimoto and Dr. Miako Sakaguchi for their assistance and advices in molecular phylogeny. We are grateful to Dr. Jeremy Pickett-Heaps for taking movie images of *H. arenicola*. This research was supported in part by Japan Society for the Promotion of Sciences (JSPS) Grants RFTF00L0162 (to I.I.) and 1612007 (to N.O.). N.O. was also supported by a JSPS Research Fellowship for Young Scientists as a JSPS Research Fellow.

Appendix A. Supplementary materials

Supplementary data associated with this article can be found in the online version at doi:10.1016/j.protis.2006.05.011

References

Andersson JO, Roger AJ (2002) A cyanobacterial gene in nonphotosynthetic protists—an early chloroplast acquisition in eukaryotes? Curr Biol **12**: 115—119

Archibald JM, Rogers MB, Toop M, Ishida K, Keeling PJ (2003) Lateral gene transfer and the evolution of plastid-targeted proteins in the secondary plastid-containing alga *Bigelowiella natans*. Proc Natl Acad Sci USA **100**: 7678—7683

Baldauf SL (2003) The deep roots of eukaryotes. Science **300**: 1703—1706

Baldauf SL, Roger AJ, Wenk-Siefert I, Doolittle WF (2000) A kingdom-level phylogeny of eukaryotes based on combined protein data. Science **290**: 972—977

Bapteste E, Brinkmann H, Lee JA, Moore DV, Sensen CW, Gordon P, Durufle L, Gaasterland T, Lopez P, Muller M, Philippe H (2002) The analysis of 100 genes supports the grouping of three highly divergent amoebae: *Dictyostelium, Entamoeba, and Mastigamoeba*. Proc Natl Acad Sci USA **99**: 1414—1419

Bhattacharya D, Yoon HS, Hackett JD (2004) Photosynthetic eukaryotes unite: endosymbiosis connects the dots. Bioessays **26**: 50—60

Butcher RW (1967) An Introductory Account of the Smaller Algae of British Coastal Waters. 4. Cryptophyceae. Fishery Investigations, Series IV. HMSO, London

Cavalier-Smith T (2003) Genomic reduction and evolution of novel genetic membranes and protein-targeting machinery in eukaryote—eukaryote chimaeras (meta-algae). Philos Trans R Soc Lond B **358**: 109—133

Chesnick JM, Cox ER (1987) Synchronized sexuality of an algal symbiont and its dinoflagellate host, *Peridinium balticum* (Levander) Lemmermann. BioSystems **21**: 69—78

Chesnick JM, Cox ER (1989) Fertilization and zygote development in the binucleate dinoflagellate *Peridinium balticum* (Pyrrhophyta). Am J Bot **76**: 1060—1072

Chesnick JM, Kooistra WHCF, Wellbrock U, Medlin LK (1997) Ribosomal RNA analysis indicates a benthic pennate diatom ancestry for the endosymbionts of the dinoflagellates *Peridinium foliaceum* and *Peridinium balticum* (Pyrrhophyta). J Eukaryot Microbiol **44**: 314—320

Clay BL, Kugrens P (1999a) Description and ultrastructure of *Kathablepharis tenuis* sp. nov. and *K. obesa* sp. nov. — two new freshwater *Kathablepharis* (Kathablepharididae) from Colorado Wyoming. Europ J Protistol **35**: 435—447

Clay BL, Kugrens P (1999b) Systematics of the enigmatic Kathablepharids, including EM characterization of the type species, *Kathablepharis phoenikoston*, and new observations on *K. remigera* comb. nov. Protist **150**: 43—59

Daugbjerg N, Hansen G, Larsen J, Moestrup Ø (2000) Phylogeny of some of the major genera of dinoflagellates based on ultrastructure and partial LSU rDNA sequence data, including the erection of three new genera of unarmoured dinoflagellates. Phycologia **39**: 302—317

Dodge JD (1971) A dinoflagellate with both a mesokaryotic and a eukaryotic nucleus. Protoplasma **73**: 145—157

Douglas S, Zauner S, Fraunholz M, Beaton M, Penny S, Deng LT, Wu XN, Reith M, Cavalier-Smith T, Maier UG (2001) The highly reduced genome of an enslaved algal nucleus. Nature **410**: 1091—1096

Elbrächter M, Schnepf E (1996) *Gymnodinium chlorophorum*, a new, green, bloom-forming dinoflagellate (Gymnodiniales, Dinophyceae) with a vestigial prasinophyte endosymbiont. Phycologia **35**: 381—393

Eschbach S, Speth V, Hansmann P, Sitte P (1990) Freeze-fracture study of the single membrane between host cell and endocytobiont in the dinoflagellates *Glenodinium foliaceum* and *Peridinium balticum*. J Phycol **26**: 324—328

Falkowski PG, Katz ME, Knoll AH, Quigg A, Raven JA, Schofield O, Taylor FJR (2004) The evolution of modern eukaryotic phytoplankton. Science **305**: 354—360

Fields SD, Rhodes RG (1991) Ingestion and retention of *Chroomonas* spp (Cryptophyceae) by *Gymnodinium acidotum* (Dinophyceae). J Phycol **27**: 525—529

Gilson PR, Su V, Slamovits CH, Reith ME, Keeling PJ, McFadden GI (2006) Complete nucleotide sequence of the chlorarachniophyte nucleomorph: Nature's smallest nucleus. Proc Natl Acad Sci USA **103**: 9566—9571

Graham LE, Wilcox LW (2000) Algae. Prentice-Hall, NJ

Gualtieri P (2001) Morphology of photoreceptor systems in microalgae. Micron **32**: 411—426

Hackett JD, Anderson DM, Erdner DL, Bhattacharya D (2004a) Dinoflagellates: a remarkable evolutionary experiment. Am J Bot **91**: 1523—1534

Hackett JD, Yoon HS, Soares MB, Bonaldo MF, Casavant TL, Scheetz TE, Nosenko T, Bhattacharya D (2004b) Migration of the plastid genome to the nucleus in a peridinin dinoflagellate. Curr Biol **14**: 213—218

Hashimoto H (2005) The ultrastructural features and division of secondary plastids. J Plant Res **118**: 163—172

Horiguchi T, Pienaar RN (1992) *Amphidinium latum* (Dinophyceae), a sand-dwelling dinoflagellate feeding on cryptomonads. Jpn J Phycol (Sorui) **40**: 353—363

Huang CY, Ayliffe MA, Timmis JN (2003) Direct measurement of the transfer rate of chloroplast DNA into the nucleus. Nature **422**: 72—76

Inagaki Y, Dacks JB, Doolittle WF, Watanabe KI, Ohama T (2000) Evolutionary relationship between dinoflagellates bearing obligate diatom endosymbionts: insight into tertiary endosymbiosis. Int J Syst Evol Microbiol **50**: 2075—2081

Inouye I, Pienaar RN (1984) Light and electron microscope observation on *Nephroselmis astigmatica* sp. nov. (Prasinophyceae). Nord J Bot **4**: 409—423

Katz LA (2002) Lateral gene transfers and the evolution of eukaryotes: theories and data. Int J Syst Evol Microbiol **52**: 1893—1900

Kugrens P, Lee RE, Corliss JO (1994) Ultrastructure, biogenesis, and functions of extrusive organelles in selected non-ciliate protist. Protoplasma **181**: 164—190

Larsen J (1988) An ultrastructural study of *Amphidinium poecilochroum* (Dinophyceae), a phagotrophic dinoflagellate feeding on a small species of cryptophytes. Phycologia **27**: 366—377

Lee RE, Kugrens P (1992) Relationship between the flagellates and the ciliates. Microbiol Rev **56**: 529—542

Lee RE, Kugrens P, Mylnikov AP (1991) Feeding apparatus of the colorless flagellate *Katablepharis* (Cryptophyceae). J Phycol **27**: 725—733

Lee RE, Kugrens P, Mylnikov AP (1992) The structure of the flagellar apparatus of two strains of *Katablepharis* (Cryptophyceae). Br Phycol J **27**: 369—380

Marin B, Nowack ECM, Melkonian M (2005) A plastid in the making: evidence for a second primary endosymbiosis. Protist **156**: 425—432

Martin W (2003a) Gene transfer from organelles to the nucleus: frequent and in big chunks. Proc Natl Acad Sci USA **100**: 8612—8614

Martin W (2003b) The smoking gun of gene transfer. Nature Genet **33**: 442

Martin W, Herrmann RG (1998) Gene transfer from organelles to the nucleus: How much, what happens, and why? Plant Physiol **118**: 9—17

Martin W, Rujan T, Richly E, Hansen A, Cornelsen S, Lins T, Leister D, Stoebe B, Hasegawa M, Penny D (2002) Evolutionary analysis of *Arabidopsis*, cyanobacterial, and chloroplast genomes reveals plastid phylogeny and thousands of cyanobacterial genes in the nucleus. Proc Natl Acad Sci USA **99**: 12246—12251

McFadden GI (2001) Primary and secondary endosymbiosis and the origin of plastids. J Phycol **37**: 951—959

Melkonian M, Robenek H (1984) The Eyespot Apparatus of Flagellated Green Algae: a Critical Review. In Round FE, Chapman DJ (eds) Progress in Phycological Research, Vol. 3. Biopress Ltd., Bristol, pp 93—268

Morden CW, Sherwood AR (2002) Continued evolutionary surprises among dinoflagellates. Proc Natl Acad Sci USA **99**: 11558—11560

Moriya M, Nakayama T, Inouye I (2000) Ultrastructure and 18SrDNA sequence analysis of *Wobblia lunata* gen. et sp. nov., a new heterotrophic flagellate (stramenopiles, incertae sedis). Protist **150**: 835—846

Nozaki H, Matsuzaki M, Misumi O, Kuroiwa H, Hasegawa M, Higashiyama T, Shin T, Kohara Y, Ogasawara N, Kuroiwa T (2004) Cyanobacterial genes transmitted to the nucleus before divergence of red algae in the Chromista. J Mol Evol **59**: 103—113

Nozaki H, Matsuzaki M, Takahara M, Misumi O, Kuroiwa H, Hasegawa M, Shin-i T, Kohara Y, Ogasawara N, Kuroiwa T (2003) The phylogenetic position of red algae revealed by multiple nuclear genes from mitochondria-containing eukaryotes and an alternative hypothesis on the origin of plastids. J Mol Evol **56**: 485—497

Okamoto N, Inouye I (2005a) A secondary symbiosis in progress? Science **310**: 287

Okamoto N, Inouye I (2005b) The katablepharids are a distant sister of the Cryptophyta: a proposal of Katablepharidophyta divisio nova/Kathablepharida phylum novum based on SSU rDNA and beta tubulin phylogeny. Protist **156**: 163—179

Posada D, Crandall KA (1998) Modeltest: testing the model of DNA substitution. Bioinformatics **14**: 817—818

Schnepf E, Elbrächter M (1999) Dinophyte chloroplasts and phylogeny — a review. Grana **38**: 81—97

Simpson AGB, Roger AJ (2002) Eukaryotic evolution: Getting to the root of the problem. Curr Biol **12**: R691—R693

Skuja H (1939) Beitrag zur Algenflora Lettlands. II. Acta Hortic Bot Univ Latviensis **11/12**:41—168

Stegemann S, Hartmann S, Ruf S, Bock R (2003) High-frequency gene transfer from the chloroplast genome to the nucleus. Proc Natl Acad Sci USA **100**: 8828—8833

Swofford DL (2003) PAUP*: Phylogenetic Analysis Using Parsimony (* and other methods), Version 4.0b10. Sinauer Associates, Inc., Sunderland, MA

Tangen K, Björnland T (1981) Observations on pigments and morphology of *Gyrodinium aureolum* Hulburt, a marine dinoflagellate containing 19′-hexanoyloxyfucoxanthin as the main carotenoid. J Plankton Res **3**: 389—401

Tippit DH, Pickett-Heaps JD (1976) Apparent amitosis in the binucleate dinoflagellate *Peridinium balticum*. J Cell Sci **21**: 273—289

Tomas RN, Cox ER (1973) *Peridinium balticum* (Levander) Lemmermann, an unusual dinoflagellate with a mesocaryotic and an eukaryotic nucleus. J Phycol **9**: 91—98

van der Giezen M, Cavalier-Smith T, Martin W, Wilkins A, Doolittle WF, Allen JF, Leaver CJ, Whatley FR, Howe CJ (2003) Genomic reduction and evolution of novel genetic membranes and protein-targeting machinery in eukaryote—eukaryote chimaeras (meta-algae) — Discussion. Philos Trans R Soc Lond B **358**: 133—134

van Dooren GG, Schwartzbach SD, Osafune T, McFadden GI (2001) Translocation of proteins across the multiple membranes of complex plastids. Biochim Biophys Acta Mol Cell Res **1541**: 34—53

Vørs N (1992a) Heterotrophic amoebae, flagellates and heliozoa from the Tvärminne area, Gulf of Finland, in 1988—1990. Ophelia **36**: 1—109

Vørs N (1992b) Ultrastructure and autecology of the marine, heterotrophic flagellate *Leucocryptos marina* (Braarud) Butcher 1967 (Katablepharidaceae/Kathablepharidae), with a discussion of the genera *Leucocryptos* and *Katablepharis*/*Kathablepharis*. Europ J Protistol **28**: 369—389

Watanabe MM, Suda S, Inouye I, Sawaguchi T, Chihara M (1990) *Lepidodinium viride* gen. et sp. nov. (Gymnodiniales, Dinophyta), a green dinoflagellate with a chlorophyll *a*- and *b*-containing endosymbiont. J Phycol **26**: 741—751

Watanabe MM, Takeda Y, Sasa T, Inouye I, Suda S, Sawaguchi T, Chihara M (1987) A green dinoflagellate with chlorophylls *a* and *b*: morphology, fine structure of the chloroplast and chlorophyll composition. J Phycol **23**: 1987

Wilcox LW, Wedemayer GJ (1984) *Gymnodinium acidotum* Nygaard (Pyrrophyta), a dinoflagellate with an endosymbiotic cryptomonad. J Phycol **20**: 236—242